Experimental Identification of Dynamic Coefficients of Tilting-Pad Bearings with Active Lubrication

Jorge G. Salazar [1], **Alejandro C. Varela** [2], **Ilmar F. Santos** [3]

[1] Technical University of Denmark, 2800, Kgs. Lyngby, Denmark, jgsal@mek.dtu.dk
[2] Technical University of Denmark, 2800, Kgs. Lyngby, Denmark, acer@mek.dtu.dk
[3] Technical University of Denmark, 2800, Kgs. Lyngby, Denmark, ifs@mek.dtu.dk

Abstract

This article presents the experimental identification of the equivalent dynamic coefficients of an actively-lubricated bearing under different lubrication regimes, namely: passive (no injection flow), hybrid (constant injection flow) and feedback-controlled (variable injection flow) lubrication. The main goal is to provide an overview on the feasibility of modifying its dynamic properties via active lubrication. The pressurized oil injection flow, which enables the hybrid and the feedback-controlled lubrication regimes, is regulated by a hydraulic control system composed of a) a high pressure oil supply unit, b) servovalves, c) radial injection nozzles, d) displacement sensors and e) well-tuned digital controllers which turn the bearing static and dynamic properties controllable. A scaled-down industrial rotor, composed by a flexible rotor supported by a four rocker LBP tilting-pad journal bearing featuring active lubrication under light load conditions, is used for such a goal. The experimental identification is performed in the frequency domain by means of the measured FRFs and a finite element model of the rotor. The comparison between results under the different lubrication regimes, presented along with their expanded uncertainty, provides experimental evidence of the modification of the bearing properties via the active lubrication.

1 Introduction

Tilting-pad journal bearings (TPJB) are widely used within the industry due to their notable stability properties among the fluid-film bearing designs. Since the dynamic characteristics of a rotor-bearing system are heavily influenced by its support elements, a long effort has been made to improve the experimental characterization and theoretical prediction of the TPJB dynamic properties. Since the work developed by Lund [1] in the 1960's, it has been a common practice to describe the TPJB dynamic characteristics using a linearization of the oil film forces around the static equilibrium, resulting in a set of equivalent stiffness and damping coefficients. Lund's original work relied in assuming a common condensation frequency – at that time, the journal rotational frequency – in order to link the journal and pads degrees of freedom when performing the perturbation analysis. This assumption enabled to obtain a set of eight synchronously reduced stiffness and damping coefficients related to the journal degrees of freedom, including implicitly the contribution from the dynamics of each pad. Allaire et al. [2] expanded this approach, by introducing a pad perturbation method which included explicitly the contribution from the pad degrees of freedom. It yields the so called full set of dynamic coefficients or KC model. The full set of coefficients can be expressed in a reduced form – by previous selection of a condensation frequency – by condensing away the pad degrees of freedom and keeping only the journal ones. As a result, the system becomes undermodeled and the resulting set of reduced dynamic coefficients exhibit frequency dependency. This dependency becomes more or less significant, depending on whether there are relevant pad dynamics taking place in the analyzed frequency range. Some early [3–6] and more recent [7–9] publications have identified the mode related to the pivot flexibility as one of the most relevant ones regarding this dependency. The frequency dependency issue has been addressed by some researchers by following the approach introduced by Rouvas and Childs in [10], which involves the obtention of a set of twelve frequency independent mass, stiffness and damping coefficients for the TPJB. In this KCM model, the mass coefficients account for the hardening or softening of the bearing response in frequency domain, by assuming that such effects are proportional to the square of the condensation frequency. A throughout analysis on the implications of the KC and KCM models for the dynamic analysis at the "system level" (rotor+bearing) and "element level" (bearing) can be found in [8, 11, 12].

The advances in the field of TPJB modeling are inherently related to the comparison between theoretical and experimental results. Nowadays, the state-of-the-art regarding the TPJB modeling establishes the need for including several effects to achieve a sufficient level of accuracy. Namely, the hydrodynamic effect due to the oil film pressure build-up, the thermal effects related to the oil film temperature build-up and the heat transfer to the bearing pads, and the flexibility effects associated with the pads and pivots elastic deformations due to the loads exerted over them. The usage of the elastothermohydrodynamic (ETHD) lubrication regime as the modeling standard is the result of the work of a long list of authors, such as Ettles [13, 14], Brockwell and Dmochowski [15], Fillon et al. [16, 17], Kim and Palazzolo [18, 19], among others.

The dynamic properties of the standard TPJB design are determined by its geometry, oil properties and operational conditions such as the applied load and the journal angular speed. Since all of these parameters are defined at the early design stage, there is no option to control the dynamic properties once the machine is in service. In order to include some parameters that could be adjusted during the machine operation with the resulting modification of its dynamic coefficients, an interest in re-design the standard TPJB has raised aimed at adjusting the whole rotor dynamic behavior. Santos [20] proposed two different designs of TPJB that featured controllable characteristics based on hydraulic actuators, to wit; the hydraulic chamber system and the hydraulic radial oil injection system or active lubrication system. The present work is focused on a TPJB design that includes an active lubrication system, also known as actively-lubricated bearing (ALB). This system involves the injection of pressurized oil into the bearing clearance through a nozzle placed in radial holes drilled across the pad, normally one in the middle of the pad surface. The injection pressure is controlled by means of a servolvalve, resulting in a modification of the oil film pressure field and the resulting forces over the rotor. Therefore, it is possible to apply controllable forces over the rotor and to adjust the bearing dynamic coefficients during the machine operation. The mathematical model formulation for the ALB follows the conventional TPJB modeling and it has been expanded to achieve a complete ETHD formulation [21, 22]. The capability of such model to predict the static and thermal behavior of the controllable bearing was evaluated in [23] by direct comparison with experimental results, yielding good results. On the other hand, the capability of the available model to predict the dynamic properties of the controllable bearing is currently under research. Most of the experimental work related to the application of the ALB has been performed using a "system level" approach, showing the feasibility of modifying the frequency response function of a flexible rotor supported by this type of bearing [24, 25]. With regards to the "element level" approach, there is a single publication related to the identification and modification of the dynamic coefficients of an ALB [26]. Therein, a comparison between theoretical and experimentally obtained dynamic coefficients was presented, using the model available at that time, i.e. rigid pad, controllable hydrodynamic isothermal model. An important underestimation in the predicted damping coefficients due to the neglection of thermal and pad flexibility effects was then obtained as an outcome.

To work at the "element level", a bearing properties identification procedure is needed. Two different coefficients identification methods, classified according to the test rig configuration employed, can be found in the literature. Namely, a) The "shake the bearing" setup, introduced originally by Glienicke [27] and extensively used by Brockwell and Kleinbub [28], Ha and Yang [29], Dmochowski [7], Childs and Carter [30], Childs and Kulhanek [31], in which the bearing is floating around a rigid rotating shaft and b) The "shake the shaft" setup, corresponding to the case where the rotating shaft moves inside a bearing whose housing is rigidly supported and used only in few investigations related to controllable bearings developed by Santos [26, 32]. With regards to the experimental contributions in the field, a complete review of a long list of contributions can be found in [33, 34]. At the same time, the procedures for obtaining the linearized dynamic coefficients from the experimental measurements can be divided in time domain and frequency domain techniques. Time domain techniques [28, 29] are not considered in this work because they are constrained to single frequency excitations besides of they also present some noise contamination issues. Instead, the frequency domain techniques which present better noise rejection characteristics are used. Such an approach allows for multifrequency excitations, an effective way of dealing with the experimental measurement of complex valued impedance functions. By using these techniques, the dynamic characteristics of the bearing can be determined simultaneously in a broad frequency range, as it is shown by Dmochowski [7] and Childs [30, 31] among others.

The main objective of this work is to experimentally demonstrate the feasibility of modifying the ALB bearing dynamic properties by using the active lubrication system enabling the so called hybrid and feedback-controlled lubrication regimes. It is out of the scope of the work to present the well known dependency of such properties on the journal angular velocity and the bearing applied load. For the goal of the work, a scaled-down rotor, close to an industrial application of the active lubrication and already used in other works [35, 36], is utilized under light load conditions. Since the ALB bearing properties exhibit frequency dependency, the experimental identification procedure is carried out in frequency domain following the approach presented in [37] which allows the usage of
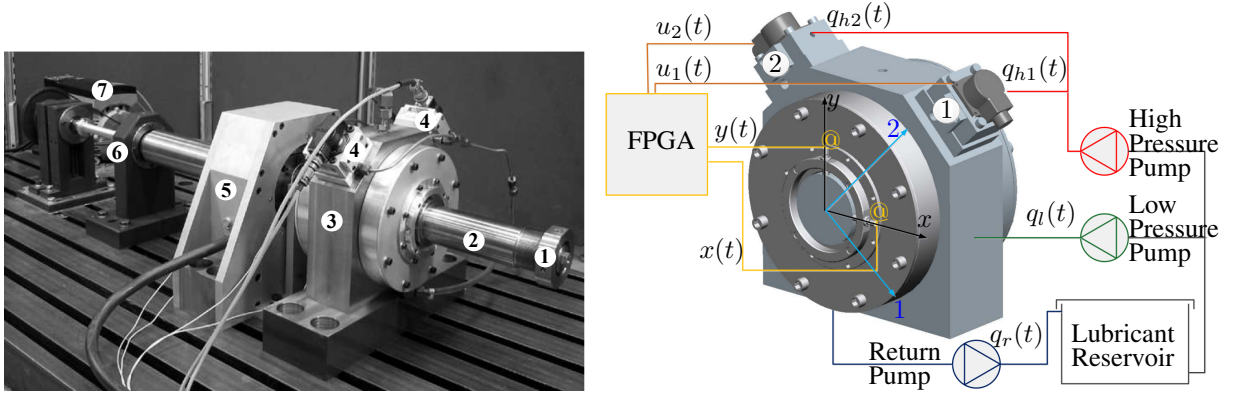
Figure 1: Flexible rotor - ALB bearing test-rig. Left: picture of the test-rig and its main components. ① The excitation bearing, ② The flexible shaft, ③ The actively lubricated bearing (ALB), ④ Servovalves, ⑤ The active magnetic bearing, ⑥ The ball bearing, ⑦ The AC motor with frequency driver. Right: A scheme of the radial oil injection control system overlapped to the ALB with its main parts, the high pressure supply unit, the servovalves ① and ②, proximity sensors @ and the digital controller (FPGA). Low pressure and return pumping units as well as the fixed orthogonal reference frames "$x - y$" and "$1 - 2$" are also included.

a finite element representation in order to properly account for the shaft flexibility contribution. A computational procedure which makes use of the same finite element model as proposed by [38] is used to compute, by means of the root-sum-square (RSS) method, the expanded uncertainty in the results.

2 Experimental Facilities. The Flexible Rotor - ALB Bearing Test-Rig

The test stand, is depicted in Figure 1. It comprises a shaft ②, with a mass of approx. 50 kg and 1150 mm long, supported by an actively-lubricated bearing (ALB) ③ and rigidly supported by a ball bearing ⑥ at its driven end. The test stand is belt-driven by means of a layshaft flexibly coupled to it. The power is supplied by a 4 HP AC motor ⑦ which by means of a frequency converter enables the test stand to run up to 7000 rpm. An active magnetic bearing ⑤ is currently mounted between bearings to exert either static and dynamic loads over the rotor in all possible directions without any mechanical link to it. Two ways of exciting the test stand are currently enabled to carry out model parameter identification. The first one, by means of the active magnetic bearing and the second one, by an excitation bearing ① placed at the free end through which unidirectional forces can be applied either by connecting an electromagnetic shaker or by carrying out impact tests. The ALB is a tilting-pad journal bearing with 4 bronze pads in a load between pads (LBP) configuration. The pads are rocker pivoted in the circumferential middle of the pad, i.e. with an offset of 0.5. The controllable or active feature of the bearing is developed by an hydraulic radial oil injection system as proposed by Santos [39]. This injection system superimposes the hydrostatic pressure on top of the hydrodynamic pressure distribution by injecting pressurized oil between the journal-pad clearance, for the current design, through a nozzle placed in the pad middle. The high

Table 1: Conventional and controllable design parameters of the actively-lubricated bearing (ALB).

Conventional Design Parameters	Value	Units	Controllable Design Parameters	Value	Units
Journal radius (R)	49.89	mm	Servovalve type	MOOG E760-912	-
Pad inner radius (R_p)	50	mm	Servovalve configuration	4 way, spool valve	-
Pad aperture angle (α_p)	69	°	Cut-off frequency (210 bar)	350	Hz
Pad width (L)	100	mm	Damping (210 bar)	0.7	-
Pad thickness (t)	14	mm	Cut-off frequency (100 bar)	260	Hz
Nominal radial clearance	110	μm	Injection orifice diameter (d_0)	3.3	mm
Assembly radial clearance	83	μm	Injection orifice length (L_0)	21	mm
Lubrication oil type	ISO VG22	-			
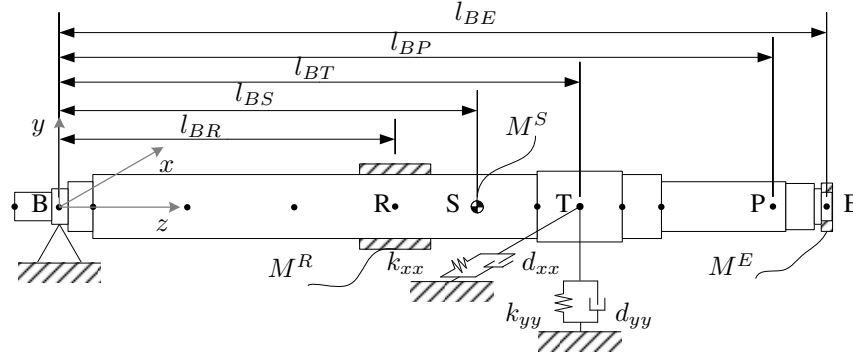
Figure 2: Schematic of the flexible rotor - ALB bearing test-rig depicting the finite element discretization. The inertial reference frame – xyz – is included. Notice that the cross-terms of the bearing coefficients have been omitted for simplicity.

pressure oil flow is controlled by two high-frequency response servovalves installed orthogonally $\pm 45°$ with the vertical direction, aligned with the "1-2" reference frame. Each servovalve is coupled to a pair of counter pads. The lubricant is supplied for the conventional and for the active lubrication by a low pressure (max. 2 bar) and a high pressure (max. 100 bar) pumping unit, respectively. Figure 1 also depicts a scheme of the radial oil injection system overlapped to a 3D drawing of the active bearing. Proximity probes, aligned with the "x-y" reference frame, used for monitoring and feeding back controllers are also included. Further design parameters can be found in Table 1 in which the conventional and controllable design parameters have been gathered apart. The test stand allows for studying the dynamic behavior of flexible rotor-ALB bearing systems when different feedback-controlled lubrication regimes are developed with the ALB. The active bearing is capable to operate under three different lubrication regimes which are discussed later in section 4.1.

3 Dynamic Coefficients Identification

The available test setup allows for a frequency domain identification based on the "shake the shaft" configuration. As a first step to perform the identification, a mathematical model capable of representing the relevant rotor-bearing system dynamics must be formulated. Depending on the frequency range where the identification takes place, two alternatives arise. Firstly, one could model the shaft as a rigid body, based on the assumption that flexibility effects have a negligible contribution in the low frequency range. Such approach is presented in [40], based on the method proposed by [41], which allows to obtain the eight linearized oil film bearing coefficients by direct comparison of the experimental FRFs against the theoretical ones. Examples of its application can be found in the same reference [40] applied to cylindrical and tilting-pad journal bearings, and in [42] and [43] applied to air foil journal bearings and polymer faced tilting-pad journal bearings, respectively.

In order to do not underestimate the bearing stiffness at low frequencies and to extend the frequency range where the identification of the bearing coefficients is possible, it becomes necessary to include the shaft flexibility effects into the mathematical model. The finite element method [44] is a well established tool for including flexibility effects in a straightforward manner. However, from a system identification point of view, this kind of mathematical model increases substantially the number of degrees of freedom of the system, preventing the experimental obtention of every possible input/output relationship. This difficulty can be overcome by applying the method presented in [37], which allows the inclusion of the shaft flexibility and to identify unknown dynamics from a reduced number of input/output relationships. The method is detailed in the following section 3.2 for the sake of completeness. Nevertheless, the reader is advised to refer to [37] for a comprehensive presentation of the method.

3.1 Mathematical Modeling of the Test-rig

The mathematical modeling of the system is based on a discretization with 21 finite elements of the shaft depicted in the schematic of Figure 2 in which some representative nodes are marked as black dots. The model accounts for the inertia and flexibility effects of the shaft, while its damping contribution is neglected. The relevant nodes for the identification procedure are identified as point (B) for the ball bearing, point (R) for the active magnetic bearing rotor, point (S) for the shaft center of mass, point (T) for the placement of the ALB, point (P) for

the placement of the sensor and point (E) for the excitation bearing. Main distances are also depicted and defined as l_{ij} for which the subscripts stand for the distance between points i and j. Concentrated masses are identified as M^R and M^E for the active magnetic bearing rotor and the excitation bearing respectively and placed in their respective nodes. The shaft mass M^S is distributed along its nodes. The mean value of these parameters are given further in Table 3 along with their uncertainty information. The finite elements implementation uses the matrices given by Lalanne [45] adapted to the used inertial reference frame – xyz – also depicted in the schematic.

3.2 Identification Procedure in the Frequency Domain

The procedure is aimed at obtaining the equivalent bearing complex impedance function $[\mathbf{H}(i\omega)]$ by means of measured frequency response functions $[\mathbf{FRF}^*(i\omega)]$ and the equivalent mathematical model of the test setup. In general terms, the test setup can be dynamically described around an equilibrium position by the well known equation of motion written in generalized coordinates as follows:

$$[\mathbf{M}]\{\ddot{\mathbf{q}}\} + ([\mathbf{D}_b] - \Omega[\mathbf{G}])\{\dot{\mathbf{q}}\} + ([\mathbf{K}] + [\mathbf{K}_b])\{\mathbf{q}\} = \{\mathbf{f}\} \tag{1}$$

where, in the matrix equation system of Equation (1), $[\mathbf{M}]$ stands for the generalized inertia matrix, $[\mathbf{G}]$ for the gyroscopic matrix, $[\mathbf{K}]$ for the stiffness matrix and $\{\mathbf{f}\}$ and $\{\mathbf{q}\}$ represent the generalized external force and displacement coordinate, respectively. Ω denotes the angular velocity. The contribution from the studied ALB bearing in terms of stiffness $[\mathbf{K}_b(\omega)]$ and damping $[\mathbf{D}_b(\omega)]$ is to be determined. Under the assumption of a linear system and considering an harmonic excitation $\{\mathbf{f}(t)\}$ of frequency ω, the generalized coordinate $\{\mathbf{q}(t)\}$ and its time derivatives are dominated by an harmonic response at the same frequency, hence they can be written using complex notation as:

$$\{\mathbf{f}(t)\} = \{\mathbf{f_0}\}e^{i\omega t}; \qquad \{\mathbf{q}(t)\} = \{\mathbf{q_0}\}e^{i\omega t}; \qquad \{\dot{\mathbf{q}}(t)\} = i\omega\{\mathbf{q_0}\}e^{i\omega t}; \qquad \{\ddot{\mathbf{q}}(t)\} = -\omega^2\{\mathbf{q_0}\}e^{i\omega t} \tag{2}$$

Replacing the expressions of Equation (2) into Equation (1), in which "i" stands for the complex unit, sorting and canceling out the exponential term, Equation (1) can be rewritten as:

$$\left[-\omega^2[\mathbf{M}] + i\omega([\mathbf{D}_b(\omega)] - \Omega[\mathbf{G}]) + [\mathbf{K}] + [\mathbf{K}_b(\omega)]\right]^{-1}\{\mathbf{f_0}\} = \{\mathbf{q_0}\}$$
$$[\mathbf{Z}_0 + \mathbf{H}_b(i\omega)]^{-1} = [\mathbf{FRF}(i\omega)] \tag{3}$$

Equation (3) states the relationship between the system dynamic stiffness matrix $[\mathbf{Z}_0]$ from the finite element model, the unknown bearing impedance function $[\mathbf{H}_b(i\omega)] = [\mathbf{K}_b(\omega)] + i\omega[\mathbf{D}_b(\omega)]$ and the matrix $[\mathbf{FRF}(i\omega)]$ containing the input/output relationships for every degree of freedom in the finite element model. Experimentally, it is not possible to determine every component of this matrix, hence some additional technique must be applied. Following the method introduced in [37], which introduced the usage of selector matrices $[\mathbf{S}_i]$ to deal only with several excited/sampled locations, the bearing impedance function $[\mathbf{H}_b(i\omega)]$ can be determined by:

$$[\mathbf{H}_b(i\omega)] = \left[[\mathbf{S}_T]^T[\mathbf{Z}_0]^{-1}[\mathbf{S}_E]\left([\mathbf{S}_P]^T[\mathbf{Z}_0]^{-1}[\mathbf{S}_E] - [\mathbf{FRF}^*(i\omega)]\right)^{-1}[\mathbf{S}_P]^T[\mathbf{Z}_0]^{-1}[\mathbf{S}_T] - [\mathbf{S}_T]^T[\mathbf{Z}_0]^{-1}[\mathbf{S}_T]\right]^{-1} \tag{4}$$

where in Equation (4), $[\mathbf{S}_E]$ stands for the selector matrix associated to the excited degrees of freedom (point E), $[\mathbf{S}_P]$ stands for the measured degrees of freedom (point P) and $[\mathbf{S}_T]$ stands for the bearing degrees of freedom (point T). The required experimental data is significantly reduced from N dof to 2 dof, since the main requirement to apply the method is that the number of excitations and sensors match the dimension of the unmodeled bearing dynamics. Hence the reduced measured FRFs matrix $[\mathbf{FRF}^*(i\omega)]$ only contains the transfer functions between the excitation point (E) and the response at the measurement point (P). As aforementioned, more details are given in [37]. From Equation (4) the bearing dynamic properties are obtained as the real and imaginary parts of the bearing impedance which reads:

$$[\mathbf{K}_b] = \Re\{[\mathbf{H}_b(i\omega)]\}; \qquad [\mathbf{D}_b] = \frac{\Im\{[\mathbf{H}_b(i\omega)]\}}{\omega} \tag{5}$$

4   Experimental Procedure

In order to identify equivalent bearing dynamic coefficients a baseline operational condition must be set. An angular velocity of 3000 rpm and an almost null resulting applied load over the bearing have been defined with the aid of the magnetic bearing. Such conditions have been selected with the intention of mimicking a rotor under light load condition. A supply pressure of 90 bar has been set for the active control system, such a relative high pressure is defined in order to make more notorious the hydrostatic effect in the bearing and keep the cut-off frequency of the servovalves out of the frequency range of study (260 Hz with approx. 100 bar). For each of the lubrication regimes featured, the test-rig is run until it reaches its thermal and geometrical steady-state equilibria before to perform the dynamic tests. These lubrication regimes are explained next.

The dynamic tests for obtaining the experimental FRFs are carry out with the aid of an electromagnetic shaker by sweeping a sinusoidal signal in the frequency range of interest. The used test setup configuration entails that the dynamic forces are exerted in the excitation bearing (point E) and the system response is measured in the proximity probe location (point P).

4.1   The Three Lubrication Regimes

The ALB bearing is capable to operate under three different lubrication regimes, namely:

The passive regime: is the lubrication regime governing all fluid film bearings due to the hydrodynamic effect developed by the pressure build up and it gives the backup support in terms of the load carrying capacity in case of an injection system failure.

The hybrid lubrication regime: is a combination of the passive case with an hydrostatic effect developed by injecting pressurized oil into the journal-pad clearance added by the injection system. Since the bearing is a four pads arrangement in a LBP configuration and governed by two servovalves, with slightly different dynamic properties, the journal can be moved in two directions within a plane. However, due to the aforementioned reasons when the oil is injected from, for instance, the two bottom/upper pads, the shaft is not moved strictly upward/downward unless an I-controller is used for positioning the shaft in the desired position [36]. Moreover, an undesired movement in the opposite orthogonal direction (left or right) is obtained. In this work the upward and downward injection cases are aided by an I-controller with k_i=-30 kV/ms, so it can ensure that the journal is being moved only in the vertical direction. For a pressure of 90 bar the maximum displacement in the vertical direction from the equilibrium position is +15μm upward and -30μm downward. When no injection scheme is set for the hybrid case, there is still some hydrostatic pressure added as a consequence of the leakage flow, due to the underlapped design of the servovalves. For descriptive purpose of this hybrid lubrication regime, this baseline case is called the leakage case.

The feedback-controlled lubrication regime, is one step further from the hybrid case and herein the injection flow and hence the hydrostatic effect is controlled dynamically by the servovalves and well-tuned digital controllers, commonly implemented in a FPGA or similar hardware with real time processing capabilities. Different control strategies can be defined considering classical or modern control design strategies based on model-free [35] or model-based system characterizations. For simplicity, the one utilized in this work is based on a basic proportional-derivative (PD) controller whose gains have been experimentally and manually tuned. For doing so, it is assumed that the test rig behaves like a stable linear time invariant system. The way to tune (synthesize) these gains is basically by defining a stable area in the parameter space ($k_p \times k_d$) by slowly varying these gains from zero until the unstable behavior of the system is reached. This tuning should start with the proportional gain k_p followed by the derivative gain k_d to then select appropriate values from the stable area. Since the simplest representation of the test rig is a two-input two-output plant, the gain synthesis is a bit challenging and depending on the control law up to 8 different gains could be necessary to determine. However if an appropriate approach is chosen, then only a pair of gains must be determined and even the same tuning methods for the single-input single-output plants can be applied. More details are given in [35]. Two sort of control laws are implemented based on a PD-controller and a P-controller. These control laws are presented below and their gain values are summarized in Table 2 together with the main parameters which define all the lubrication regimes used in the present work.

4.2   Control Laws for the Feedback-Controlled Lubrication Regimes

Control Law #1 If the simplest control law is considered, only a pair of control gains (k_p, k_d) must be determined. Despite of such advantage, an important drawback is obtained by using the same control gains to govern both servovalves since their dynamics cannot be managed independently. The control signals $\{u_1 \ u_2\}^T$ can be

obtained in terms of the measured displacement as [35]:

$$\begin{Bmatrix} u_1 \\ u_2 \end{Bmatrix} = -k_p \begin{bmatrix} 1 & 1 \\ -1 & 1 \end{bmatrix} \begin{Bmatrix} x \\ y \end{Bmatrix} - k_d \begin{bmatrix} 1 & 1 \\ -1 & 1 \end{bmatrix} \begin{Bmatrix} \dot{x} \\ \dot{y} \end{Bmatrix} \qquad (6)$$

where in Equation (6), $\{x \; y\}^T$ and $\{\dot{x} \; \dot{y}\}^T$ stand for the feedback control signals of rotor lateral displacement and velocity respectively. To determine the velocity signals, the displacement signals are low-pass filtered and then numerically differentiated. Under the assumption of a frequency independent relationship between the control signals and the active forces, i.e. a negligible dynamic contribution of the hydraulic control system in the frequency range, it can be shown that by using the control law #1 the most influenced terms of the dynamic coefficients are the cross-terms rather than the direct ones. Although the effect of increasing the cross-terms does not lead to any benefit to the bearing, this simplest control law is considered since it is in line with the goal of the work.

Control Law #2: A more aggressive control law can be chosen for modifying the direct-terms of the dynamic coefficients. However, additional gains for the PD-controller must be determined. If the following control law is used, which only considers the proportional action, then a pair of proportional gains (k_{p_1}, k_{p_2}) for the P-controller must be synthesized. This control law #2 allows to command the servovalves in terms of the control feedback signals weighted independently, then it can be written as:

$$\begin{Bmatrix} u_1 \\ u_2 \end{Bmatrix} = - \begin{bmatrix} k_{p_1} & k_{p_2} \\ rk_{p_1} & -k_{p_2} \end{bmatrix} \begin{Bmatrix} x \\ y \end{Bmatrix} \qquad (7)$$

where in Equation (7) r is a constant identified in the experimental gain matrix which relates the control signals with the active forces. It can be demonstrated, under the same assumption of a frequency independent relationship between the control signals and the active forces, that each gain k_{p_i} modifies the direct stiffness coefficients in each direction respectively, and that the cross stiffness coefficients are not modified. Furthermore, since the derivative gains k_{d_i} are not defined the bearing damping properties are not affected. This control law can be beneficial for the rotor-bearing system since it can be used to increase the asymmetry of the bearing direct-terms while not affecting the cross-terms.

5 Identified Dynamic Coefficients for the ALB

The bearing dynamic coefficients were identified in the frequency range between 15-130 Hz. In the following, the uncertainty analysis and then the results for the different lubrication regimes are presented.

5.1 Uncertainty Analysis

The inclusion of the uncertainty in experimental results, in this case in the bearing dynamic properties, gives an estimate of the interval (normally, with 95% of confidence) on which the results are thought to lie. Guidelines to the treatment of the uncertainty analysis in experimental results are given by ANSI/ASME PTC-19.1 [46] and ISO GUM [47] standards. The measurement random uncertainties in the measured FRFs are treated considering a

Table 2: Main parameters for the lubrication regimes featured with the ALB bearing.

Lub. Regime	Ω [rpm]	P_{inj} [bar]	Injection	PD-controller #1 k_p [kV/m]	k_d [Vs/m]	P-controller #2 k_{p_1}/k_{p_2} [kV/m]
Passive	3000	-	-	-	-	-
Hybrid	3000	90	Leakage	-	-	-
Hybrid	3000	90	Upwd(15μm)	-	-	-
Hybrid	3000	90	Dwnwd(30μm)	-	-	-
Active #1	3000	90	-	$\pm$30	-	-
Active #1	3000	90	-	$\pm$30	$\pm$20	-
Active #2	3000	90	-	-	-	$\pm$30/$\pm$30

large amount of averages in order to minimize their standard deviation and to work with their mean values as their best estimates. With such an approach, it is considered that random uncertainties are not influencing the results and this work only accounts for measurement and modeling systematic uncertainties. Referring to Equation (1) the modeling uncertainties arise from the determination of the system mass $[\mathbf{M}]$, gyroscopic $[\mathbf{G}]$ and stiffness $[\mathbf{K}]$ matrices, i.e. masses and inertias of the system, and from the lengths of the finite elements as well. The uncertainty in the journal angular velocity Ω is not considered. The total uncertainty of the identified coefficients is calculated as proposed by [38] and following the ISO GUM [47] recommendations for the treatment of systematic uncertainties of type B. Table 3 summarizes all the parameters considered for the evaluation of the uncertainty along with their mean values, sources, error limits and standard uncertainties. Uncertainties in the inertia were evaluated considering the uncertainties in their respective radius of mean value A. For the measured parameters their error limits where obtained from their instruments whilst for the case of parameters obtained from CAD files their error were estimated lower that 1%. In the case of estimated radius a bigger error of 3% was considered. A normal distribution with 95% of interval confidence level is considered for all parameters, except for the measured ones, for which a uniform distribution with 100% interval confidence level is considered. Regarding the transducers, the load cell manufacturer informs linearity of $\pm1\%$ at maximum load while for the proximity probe no information was obtained. However, a linearity of $\pm3\%$ was estimated based on a similar transducer type. For both source of uncertainties a normal distribution with 95 % of confidence level was considered. Finally, a normal distribution with a confidence level of 95% is considered to calculate the confidence limits or expanded uncertainty in the results.

A simple Pareto chart shows that the parameters which contribute the most to the total uncertainty are the transducer sensitivities and lengths. In particular the sensitivity of the displacement sensor and the distances from the ALB bearing, the proximity probe and from the excitation bearing to the ball bearing. In general, acceptable values of the expanded uncertainties were obtained, below $\pm17\%$, however for some cases at low frequencies for the damping under hybrid lubrication and for some feedback-controlled cases, uncertainties within 37% and 41% were obtained.

5.2 Dynamic Coefficients of the ALB under Passive and Hybrid Lubrication Regimes
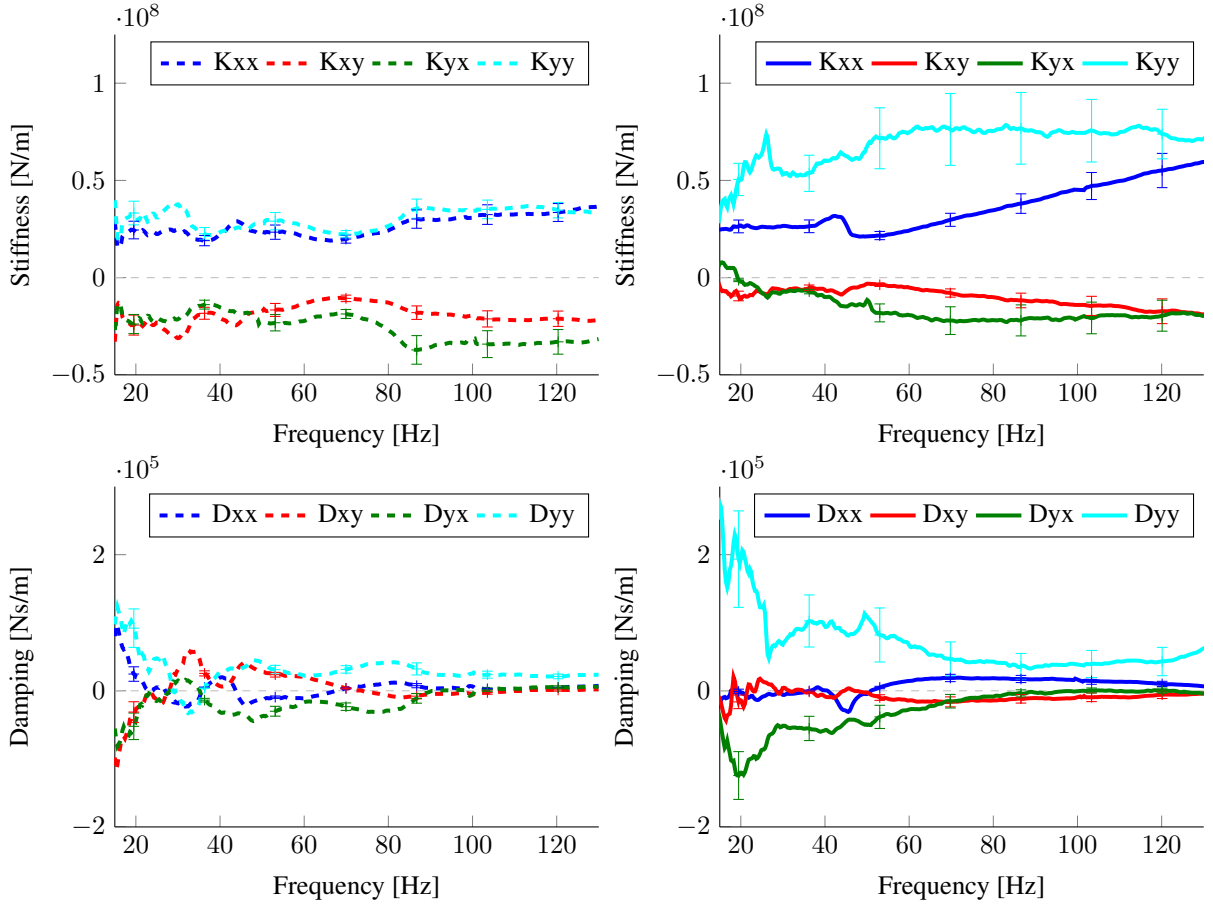
Figure 3 shows the identified dynamic coefficients for the ALB under passive and hybrid lubrication regimes in the frequency range between 15-130 Hz. If the attention is drawn over the passive case, the dashed lines, then it can be noticed for the stiffness coefficients (upper left plot) that the direct-terms are comparatively the same. Additionally, it is clear that the cross-terms are in the same order of magnitude – to the power of 10^7 – than the direct ones but negative. This can be attributable to the light load condition imposed over the rotor which leads to a low eccentricity value. In general, the identified stiffness coefficients for the passive case can be considered almost constant in the identification frequency range. With regards to the expanded uncertainty, low values are obtained with the largest one of about $\pm20\%$ for the K_{yx} term. For the damping coefficients (bottom left plot), a weak frequency dependent behavior makes more difficult to read the results, specially below 50 Hz. However, it can be stated that over 50 Hz their values are in the order of magnitude of to the power of 10^4 and that the results are little affected by the expanded uncertainty.

The right side of Figure 3 shows, in the same scale and with solid lines, the identified dynamic coefficients obtained for the hybrid case named the leakage case. Under this lubrication regime it becomes evident for the stiffness (upper right plot) that the direct-term in the vertical direction K_{yy} increase significantly its value to about $7.5 \cdot 10^7$ N/m while the direct-term in the horizontal direction K_{xx} remains within the same values, i.e., the bearing becomes more asymmetric. A strong frequency dependency after 50 Hz is seen for K_{xx}. Regarding the cross coupling terms, it can be noticed that they are reduced for the hybrid case in comparison to the passive case. The expanded uncertainty becomes more important as the frequency increases and it is far more important for the

Table 3: Model parameters considered for the uncertainty evaluation.

| Param.	Mean Value	Source	Error Limits	Standard Uncertainty	Param.	Mean Value	Source	Error Limits	Standard Uncertainty
M^S	49.55 kg	CAD file	$\pm 1\%$	± 0.2528 kg	l_{BP}	1.0015 m	Measured	± 0.005 m	0.0029 m
M^R	6.48 kg	Measured	± 0.020 kg	± 0.0115 kg	l_{BE}	1.0790 m	CAD file	$\pm 1\%$	0.00551 m
M^E	1.1124 kg	Measured	± 0.0020 kg	± 0.0112 kg	r^S	A	CAD file	$\pm 1\%$	0.01A/1.96
l_{BR}	0.4850 m	Measured	± 0.005 m	± 0.0029 m	$r^{R,E}$	A	Estimated	$\pm 3\%$	0.03A/1.96
l_{BT}	0.7315 m	CAD file	$\pm 1\%$	±0.0037 m					

Figure 3: Identified dynamic coefficients for the ALB. Left: ALB under passive lubrication regime (dashed lines (--)). Right: ALB under hybrid lubrication regime, the leakage case (solid lines (–)).

vertical direct coefficient K_{yy} with a magnitude of about $\pm17\%$. In the case of the damping coefficients (bottom right plot) it is noticed that the ALB bearing becomes more damped and that their damping properties under hybrid lubrication are strongest in the vertical direction, i.e. D_{yy}. Moreover, for all terms the damping is significantly reduced with the frequency from the power of 10^5 to the power of 10^4 over the frequency span of 60 Hz. In the horizontal direction, at low frequencies, the damping coefficients D_{xx} and D_{xy} are significantly smaller than those in the vertical direction. Over 60 Hz, D_{yy} provides the largest damping to the system while the cross-terms D_{xy} and D_{yx} are negative. The expanded uncertainty for the damping case, is more significant for the direct vertical coefficient D_{yy} at low frequencies where it reaches a $\pm37\%$ of expanded uncertainty.

5.3 A Comparison of the Identified Dynamic Coefficients under Different Hybrid Lubrication Regimes

Figure 4 depicts comparative plots of the identified dynamic properties of the ALB bearing for all hybrid lubrication regimes featured, i.e., for the leakage, upward injection and downward injection cases. Recalling that the injection cases were aided by an I-controller trying to keep the journal movement only in the vertical direction within the maximum movement allowed by the servovalves, it means, 15 μm upwards and 30 μm downwards from their equilibrium position set by the operational condition of 3000 rpm and 90 bar of high pressure supply. The leakage case, plotted in solid lines, is used as a benchmark, while the upward and downward injection cases are plotted with dotted and dashed lines respectively. Although it can be argued that all difference between them lies within the confidence limits, it is clear that the vertical direct-term K_{yy} is reduced when the shaft is moved upward, closer to the bearing center, which turns the ALB bearing more soft in the vertical direction. Another important result, is that when the injection is downwards, the cross-terms are reduced over the 50 Hz and in this case less influenced by the uncertainties. Regarding the damping, there is not big differences between the different hybrid cases and the damping terms behave almost similarly within the uncertainty bounds. Hence it can be stated that the damping is hardly affected by such lubrication conditions.
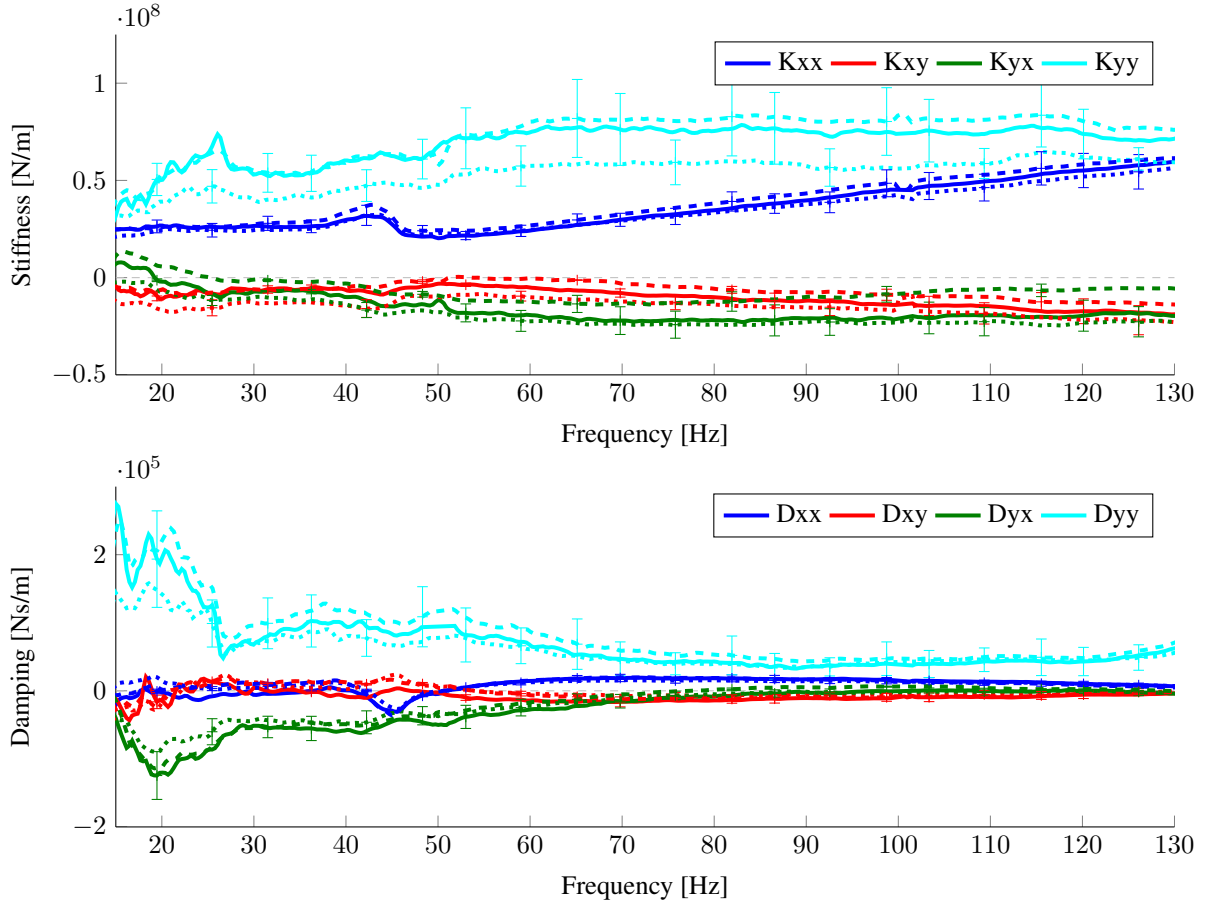
Figure 4: Comparison of the identified dynamic coefficients under the different hybrid lubrication regimes. Solid line (–): Leakage case. Dotted line (··): Upward injection aided by the I-controller. Dashed line (--): Downward injection aided by the I-controller.

5.4 Results Under Different Feedback-Controlled Lubrication Regimes

Figure 5 shows selected results for the identified coefficients under the feedback-controlled lubrication regimes in the range of 60 - 130 Hz. Left plots (dashed line) show the results obtained with the active lubrication defined by the control law #1, a PD-controller with a proportional gain of k_p=-30 kV/m and a derivative gain of k_d=20 Vs/m. Right plots (dotted line) depict the identified dynamic coefficients obtained under feedback-controlled lubrication defined by the control law #2, specifically a P-controller with gains k_{p_1}=30 kV/m and k_{p_2}=-30 kV/m. As benchmark, it has been added with thin solid lines, the coefficients obtained for the leakage case. For the PD-controller with control law #1 (dashed lines) and with regards to the stiffness coefficients (upper left plot) it can be noticed a constant behavior for the direct coefficients, even for K_{xx} which used to have a frequency dependent trend within the analyzed frequency range for the leakage case (see the thin solid line). The cross-terms, as it was earlier commented, were strongly affected in this frequency range due to the control law adopted. An important uncertainty can be seen between 60-80 Hz for both direct-terms with a maximum confidence limits of $\pm 37\%$ as well as for the term K_{yx} but with lower values in the whole analyzed frequency span. Similarly, same behavior was obtained for the damping, the direct-terms vary much more compared the leakage case and the cross-terms were affected the most. An important uncertainty is seen for the cross-terms of damping, specially between 60-80 Hz of about 40%.

In comparison to the previous results with the PD-controller, for the P-controller with control law #2 (dotted lines), it is seen that the cross-terms of the stiffness coefficients are less affected due to the control law (top right plot). The direct-terms were also affected, in fact, compared to the previous case it can be noticed an important reduction in the horizontal direct stiffness coefficient K_{xx}. On the other hand, it seems that the direct-terms are the most affected with the control law #2 as it was pursued. Damping coefficients (bottom right plot) are also modified with the control law, even though the featured controller was a P-controller, which can be demonstrated from a
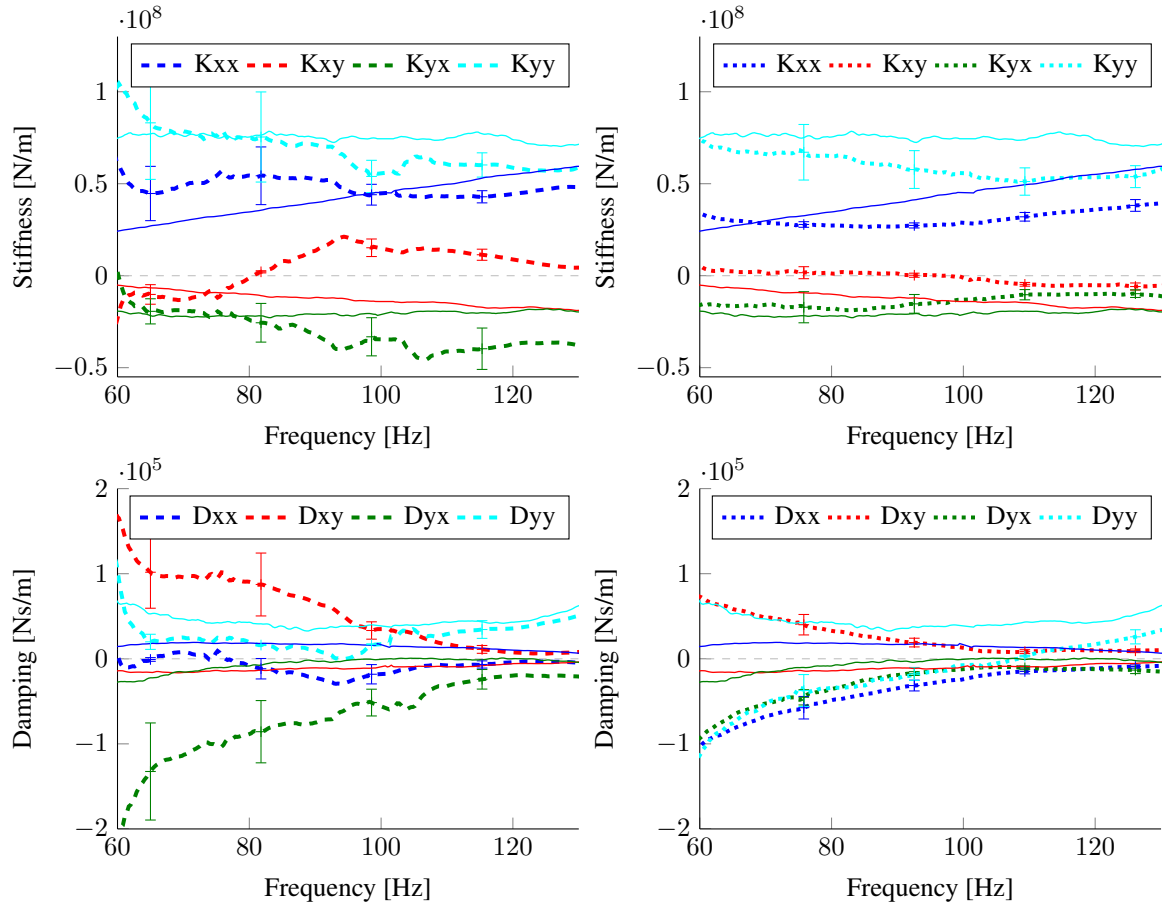
Figure 5: Identified dynamic coefficients for the ALB. Left: ALB under feedback-controlled lubrication regime, control law #1 (dashed lines (--)), k_p=-30 [kV/m] & k_d=20 [Vs/m]. Right: ALB under feedback-controlled lubrication regime, control law #2 (dotted lines (··)), k_{p_1}=30 [kV/m] & k_{p_2}=-30 [kV/m]. Results obtained under the leakage hybrid case are superposed with solid lines (–) as a benchmark.

control point of view that it only affects the stiffness properties. However, it is known that for a fluid film bearing both properties are coupled.

6 Conclusions and Future Aspects

The main contribution of the paper is of experimental nature, since no theoretical results showing the dynamic behavior of ALB bearing are presented. The comparison between theoretical and experimental results is a natural future step of the research project. In the light of the experimental investigations followed by comprehensive uncertainty analysis results obtained, one demonstrates that:

- the ALB bearing dynamic coefficients can be modified by developing the hybrid or feedback-controlled lubrication regimes. Such a modification has a big impact in the possible industrial application of the ALB bearing since it can be used to adjust the whole rotor-bearing system properties when needed.
- The identified stiffness coefficients obtained under passive lubrication illustrate an almost constant beavior in the identification frequency range.
- The hybrid lubrication regimes seem to be desirable operational regimes for the ALB bearing based on TPJB design from a stability point of view, since these regimes can increase the bearing stiffness asymmetry and contribute to reduce even more the cross-terms of this type of bearing. Furthermore, under these lubrication regimes, the ALB bearing becomes more damped.
- The hybrid lubrication regimes also allow to modify the direct stiffness of the bearing by changing the journal equilibrium position by injecting presurized oil in different direction which can be aided by I-controllers. A

softening in the vertical direction of this type of bearing – in comparison to the leakage case – can be obtained when the shaft is lifted over its equilibrium position, since the eccentricity can be significantly reduced.

• The feedback-controlled lubrication succeeded in modifying the ALB bearing properties. It was shown that this sort of lubrication regime can be developed with simple PD controllers and by choosing proper control laws can lead to beneficial modification of the bearing dynamic properties.

• The chosen control law for developing the feedback-controlled lubrication is fundamental in order to modify the bearing properties in a way that can be beneficial for the whole rotor-bearing system. It was shown that two different control laws – for this two-input two-output system – can produce dissimilar effects on the direct and cross bearing terms.

• The experimental behavior of the ALB dynamic coefficients and their dependency on the excitation frequency seem to be strongly affected by the dynamic of the foundation and hydraulic system at low frequency ranges up to 40 Hz. Given that the identification procedure is only built upon the flexible shaft dynamics, i.e., neglecting foundation and hydraulic system dynamics, the results at low frequencies should be seen as equivalent stiffness and damping of the whole rotor-bearing-foundation systems rather than of the ALB.

REFERENCES

[1] Lund, J., 1964. "Spring and Damping for the Tilting Pad Journal Bearings". *ASLE Trans., 7*(4), pp. 342–352.

[2] Allaire, P., Parsell, J., and Barrett, L., 1981. "A Pad Perturbation Method for the Dynamic Coefficients of Tilting-Pad Journal Bearings". *Wear, 72*, pp. 29–44.

[3] Klumpp, R., 1975. "A Contribution to the Theory of Tilting-Pad Bearings". PhD Thesis, University of Karlsruhe, Germany.

[4] Malcher, L., 1975. "The Stiffness and Damping Qualities of Slider Bearings for Turbomachines – Experimental Tests of MGF and Tilting Pad Bearings". PhD Thesis, University of Karlsruhe, Germany.

[5] Springer, H., 1980. "Dynamic characteristics of silding bearings with movable segments". *VDI–Berichte, 381*, November, pp. 177–184.

[6] Santos, I. F., 1993. "Active Tilting Pad Bearings – Theory and Experiment". In *VDI Fortschritt–Berichte*, Vol. 189 of *Reihe 11: Schwinsgungtechnik*. VDI Verlag.

[7] Dmochowski, W., 2007. "Dynamic Properties of Tilting-Pad Journal Bearings: Experimental and Theoretical Investigation of Frequency Effects due to Pivot Flexibility". *ASME Journal of Engineering for Gas Turbines and Power, 129*, July, pp. 865–869.

[8] Wilkes, J., and Childs, D., 2012. "Tilting Pad Journal Bearings - A Discussion on Stability Calculation, Frequency Dependence and Pad and Pivot". *ASME Journal of Engineering for Gas Turbines and Power, 134*, December.

[9] San Andres, L., and Tao, Y., 2013. "The Role of Pivot Stiffness on the Dynamic Force Coefficients of Tilting Pad Journal Bearings". *ASME Journal of Engineering for Gas Turbines and Power, 135*, November.

[10] Rouvas, C., and Childs, D., 1993. "A Parameter Identification Method for the Rotordynamic Coefficients of a High Reynolds Number Hydrostatic Bearing". *ASME Journal of Vibrations and Acoustics, 115*, pp. 264–270.

[11] Dimond, T., Younan, A., and Allaire, P., 2010. "Comparison of Tilting-Pad Journal Bearing Dynamic Full Coefficients and Reduced Order Models using Modal Analysis". *ASME Journal of Vibration and Acoustics, 132*, October, pp. 13–43.

[12] Dimond, T., Younan, A., and Allaire, P., 2012. "The Effect of Tilting Pad Journal Bearing Dynamic Models on the Linear Stability Analysis of an 8-Stage Compressor". *ASME Journal of Engineering for Gas Turbines and Power, 134*, May.

[13] Ettles, C., 1980. "The Analysis and Performance of Pivoted Pad Journal Bearings considering Thermal and Elastic Effects". *J. Lubr. Tech., ASME Trans., 102*(2), pp. 182–194.

[14] Ettles, C., 1992. "The Analysis of Pivoted Pad Journal Bearing Assemblies considering Thermoelastic Deformation and Heat Transfer Effects". *STLE Tribology Transactions, 35*(1), pp. 156–162.

[15] Brockwell, K., and Dmochowski, W., 1992. "Thermal Effects in the Tilting Pad Journal Bearing". *J.Phys.D: Appl.Phys, 25*, pp. 384–392.

[16] Fillon, M., Bligoud, J. C., and Frêne, J., 1990. "Influence of Bearing Element Displacements on Ther-

mohydrodynamic Characteristics of Tilting-Pad Journal Bearings". *Proceedings of the Japan International Tribology Conference, Nagoya 1990*, pp. 635–640.

[17] Fillon, M., Bligoud, J. C., and Frêne, J., 1992. "Experimental Study of Tilting-Pad Journal Bearings – Comparison with Theoretical Thermoelastohydrodynamic Results". *ASME Journal of Tribology,* **114**, pp. 579–588.

[18] Kim, J., Palazzolo, A., and Gadangi, R., 1994. "TEHD Analysis for Tilting Pad Journal Bearings using Upwind Finite Element Method". *Tribology Transactions,* **37**(4), pp. 771–783.

[19] Kim, J., Palazzolo, A., and Gadangi, R., 1995. "Dynamics Characteristics of TEHD Tilt Pad Journal Bearing Simulation including Multiple Mode Pad Flexibility". *ASME Journal of Vibration and Acoustics,* **117**(1), January, pp. 123–135.

[20] Santos, I. F., 1994. "Design and Evaluation of Two Types of Active Tilting Pad Journal Bearings". In *The Active Control of Vibration*, C.R.Burrows and P.S.Keogh, eds. Mechanical Engineering Publications Limited, London, England, pp. 79–87.

[21] Cerda, A., and Santos, I. F., 2012. "Performance Improvement of Tilting-Pad Journal Bearings by means of Controllable Lubrication". *Mechanics & Industry,* **13**, pp. 17–32.

[22] Cerda, A., Fillon, M., and Santos, I. F., 2012. "On the Simplifications for the Thermal Modeling of Tilting-Pad Journal Bearings under Thermoelastohydrodynamic Regime". *Proceedings of ASME Turbo Expo 2012*.

[23] Cerda, A., Bjerregaard Nielsen, B., and Santos, I. F., 2013. "Steady state characteristics of a tilting pad journal bearing with controllable lubrication: Comparison between theoretical and experimental results". *Tribology International,* **58**(1), pp. 85–97.

[24] Santos, I. F., and Scalabrin, A., 2003. "Control System Design for Active Lubrication with Theoretical and Experimental Examples". *Journal of Engineering for Gas Turbines and Power, ASME Trans.,* **125**, January, pp. 75–80.

[25] Nicoletti, R., and Santos, I. F., 2005. "Frequency Response Analysis of an Actively Lubricated Rotor/Tilting-Pad Bearing System". *ASME Journal of Engineering for Gas Turbines and Power,* **127**, July, pp. 638–645.

[26] Santos, I. F., 1996. "Theoretical and Experimental Identification on the Stiffness and Damping Coefficients of Active-Tilting Pad Journal Bearings". In *Identification in Engineering Systems*, M. Friswell and J. Mottershead, eds. The Cromwell Press Ltd., Swansea, Great Britain, pp. 325–334.

[27] Glienicke, J., 1966. "Experimental Investigation of Stiffness and Damping of Turbine Bearings and their Application to Instability Predictions". *Proc.ImechE,* **181**(3B), pp. 116–129.

[28] Brockwell, K., Kleinbub, D., and Dmochowski, W., 1989. "Measurement and Calculation of the Dynamic Operating Characteristics of the Five Shoe Tilting-Pad Journal Bearing". *STLE Tribology Transactions,* **33**(4), pp. 481–492.

[29] Ha, H., and Yang, S., 1999. "Excitation Frequency Effects on the Stiffness and Damping Coefficients of a Five Pad Tilting Pad Journal Bearing". *ASME Journal of Tribology,* **121**(3), pp. 517–522.

[30] Childs, D., and Carter, C., 2011. "Rotordynamics Characteristics of a Five Pad, Rocker-Pivot, Tilting Pad Bearing in a Load-on-Pad Configuration; Comparisons to Predictions and Load-Between-Pad Results". *ASME Journal of Engineering for Gas Turbines and Power,* **133**, August.

[31] Kulhanek, C., and Childs, D., 2012. "Measured Static and Rotordynamic Coefficients Results for a Rocker-Pivot, Tilting-Pad Bearing with 50% and 60% offsets". *ASME Journal of Engineering for Gas Turbines and Power,* **134**, May.

[32] Santos, I. F., 1993. "Active Tilting Pad Bearings - Theory and Experiment". *VDI Fortschritt-Berichte, Reihe 11: Schwingungstechnik*(189).

[33] Dimond, T., Sheth, P., Allaire, P., and He, M., 2009. "Identification methods and test results for tilting pad and fixed geometry journal bearing dynamic coefficients - A review". *Shock and Vibration,* **16**, pp. 13–43.

[34] Tiwari, R., Lees, W., and Friswell, M., 2004. "Identification of dynamic bearing parameters: a review". *Shock and Vibration Digest,* **36**(2), March, pp. 99–124.

[35] Salazar, J. G., and Santos, I. F., 2014. "Feedback-controlled lubrication for reducing the lateral vibration of flexible rotors supported by tilting-pad journal bearings". *Proc IMechE Part J: J Engineering Tribology*(In Review).

[36] Salazar, J. G., and Santos, I. F., 2014. "Exploring integral controllers in actively-lubricated tilting- pad journal bearings". *Proc IMechE Part J: J Engineering Tribology*(In Review).

[37] Wang, Q., and Maslen, E., 2006. "Identification of Frequency-Dependent Parameters in a Flexible Rotor System". *ASME Journal of Engineering for Gas Turbines and Power, 128*, July, pp. 670–676.

[38] Moffat, R., 1988. "Describing the Uncertainties in Experimental Results". *Experimental Thermal and Fluid Science, 1*, pp. 3–17.

[39] Santos, I. F., and Russo, F., 1998. "Tilting-Pad Journal Bearings with Electronic Radial Oil Injection". *Journal of Tribology, ASME Trans., 120*(3), pp. 583–594.

[40] Arumugam, P., S. S., and Prabhu, B., 1995. "Experimental identification of linearized oil film coefficients of cylindrical and tilting pads bearings". *Journal of Engineering for Gas Turbines and Power, 117*, July, pp. 593–599.

[41] Wang, J., and Liou, C., 1991. "Experimental identification of mechanical joint parameters". *Journal of Vibration and Acousics - Transactions of the ASME, 113*(1), pp. 28–36.

[42] Larsen, J. S., Hansen, A. J.-T., and Santos, I. F., 2014. "Experimental and theoretical analysis of a rigid rotor supported by air foil bearings". *Mechanics and Industry, eFirst*(11), pp. 1–13.

[43] Simmons, G. F., Cerda Varela, A. J., Santos, I., and Glavatskih, S., 2014. "Dynamic characteristics of polymer faced tilting pad journal bearings". *Tribology International, 74*, pp. 20–27.

[44] Nelson, H., and McVaugh, J., 1976. "The Dynamics of Rotor-Bearing Systems Using Finite Element". *J. Eng. Ind., 98*, pp. 593–600.

[45] Lalanne, M., and Ferraris, G., 1998. *Rotordynamics Prediction in Engineering, 2nd Edition*. Wiley.

[46] ANSI/ASME PTC-19.1, 2013. "Measurement uncertainty". ASME, New York, p. 112.

[47] ISO/IEC Guide 98-3, 2008. "Guide to the expression of uncertainty in measurement (GUM:1995)". ISO, Geneva, Switzerland, p. 120.